Copyright © 2005 American Scientific Publishers
All rights reserved
Printed in the United States of America

SENSOR LETTERS
Vol. 3, 42–48, 2005

RESEARCH ARTICLE

Sensing of Flow and Shear Stress Using Fluorescent Molecular Rotors

Mark A. Haidekker,[1,*] Walter Akers,[1] Darcy Lichlyter,[1]
Thomas P. Brady,[2] and Emmanuel A. Theodorakis[2]

[1] *Department of Biological Engineering, University of Missouri-Columbia, Columbia, MO 65211, USA*
[2] *Department of Chemistry and Biochemistry, University of California, San Diego, 9500 Gilman Drive, La Jolla, CA 92093-0358, USA*

(Received: 8 December 2004. Accepted: 13 December 2004)

Molecular rotors are fluorescent molecules with two competing pathways of deexcitation: They return from the excited singlet state to the ground state either through fluorescence or through nonradiative intramolecular rotation. Molecular rotors are known as viscosity sensors, because intramolecular rotation rate depends on the viscosity of the solvent. In this study, we describe a new observation that the emission intensity of certain molecular rotors with hydrophilic head groups is elevated in fluids under shear. This intensity increase is dependent on both fluid velocity and viscosity. Statistically significant intensity increase was observed at fluid velocities as low as 0.6 mm/s. Using fiberoptics, local flow profiles could be probed. Measuring emission intensity of molecular rotors in sheared fluids may lead to the development of new shear field sensors, allowing real-time measurement of shear and flow without disturbing the fluid.

Keywords: Viscosity, Circulation, Fluid Dynamics.

1. INTRODUCTION

Fluorescent molecules often exhibit environment-sensitive properties. Examples include sensitivity towards solvent pH, polarity, or ion concentration. A specific group of fluorescent molecules is known to form twisted intramolecular charge-transfer (TICT) states. One of the best-known representatives of this group is 4-*N*,*N*-Dimethylaminobenzonitrile (DMABN),[1] which has been shown to exhibit dual emission bands in polar environments.[2] Less known is a behavior where the twisted state leads to nonradiative decay.[3–5] Following photoexcitation, these molecules can return to the ground state via two different pathways: fluorescence emission or nonradiative intramolecular rotation. In a less viscous environment, the intramolecular rotation prevails, resulting in low fluorescence quantum yield. In a highly viscous environment the intramolecular rotation is hindered and fluorescence emission becomes the dominant deexcitation pathway. Those molecules have been commonly known under the term of molecular rotors.

It has been shown that the fluorescence quantum yield of a molecular rotor can be directly related to the solvent viscosity,[3] suggesting that these molecules can be used as nonmechanical, fluorescent viscosity sensors. Applications of this concept include sensors in polymerization processes,[6] viscosity indicators in phospholipid bilayers and the cell membrane,[6,7] probes for cytoskeletal architecture,[8,9] protein binding[10] and to measure biofluid viscosity in a nonmechanical manner.[11] One major advantage of fluorescent probes is their high spatial resolution, allowing to probe for microviscosity.[6]

This paper describes a new effect, an increase of rotor fluorescence emission in sheared fluids. It will be shown that molecular rotors exhibit markedly increased emission intensity at relatively low shear rates, and that the emission primarily depends on shear stress, not on shear rate. When fluid flows, the fluid velocity is usually not homogeneous. The spatial gradient of the velocity is called shear rate.

*Corresponding author; E-mail: HaidekkerM@missouri.edu

 1546-198X/2005/3/042/007/$17.00+.25 doi:10.1166/sl.2005.003

The product of shear rate and viscosity yields shear stress, which is the primary determinant of the forces related to the flow. Apart from numerical computations, fluid flow is primarily measured noninvasively using Doppler ultrasound, laser Doppler techniques, or magnetic resonance imaging.[12] A popular alternative is particle tracking.[13] All of these methods are limited spatially due to image resolution and particle size, respectively. Also, these methods measure fluid flow, but not fluid shear stress. This poses a limitation, because the importance of fluid shear stress in cardiovascular disease[14,15] and bone remodeling[16] has been demonstrated. Furthermore, the full implications of such an effect in biological systems cannot be efficiently evaluated due to the spatial limitations of all methods currently used. Molecular rotors could be used to directly measure shear stress with microscopic resolution, thereby offering a significant advance in real-time flow and shear stress imaging. These results give rise to the concept of a fluorescent high-resolution real-time shear stress sensor.

2. MATERIALS AND METHODS

2.1. Instrumentation

Fluorescence measurements were performed on a Fluoromax-3 spectrophotometer (Jobin-Yvon Inc., Edison, NJ) equipped either with the standard four-sample cuvette holder, which includes temperature control and a magnetic stirrer, or with a custom fiberoptic attachment that was mounted inside the sample compartment. The fiberoptic attachment consisted of an SMA-connector with collimating lens (Thorlabs Inc, Newton, NJ); a dichroic shortpass mirror ($\lambda_{50} = 465$ nm) that allowed blue excitation light to pass from the excitation monochromator to the SMA adaptor, while reflecting green emission light into the emission monochromator; and an additional 475 nm longpass filter in the emission path (mirror and filter from Chroma, Brattleboro, VT). A multimode optical fiber with 0.48 numerical aperture and 600 μm core (Thorlabs) was cut to expose the core on one end. A tip was formed by etching in 48% hydrofluoric acid (Sigma, St. Louis, MO) for two to four hours. Capillary action between the silica core and the reflective layer around the core ("cladding") tapers the tip. The process was monitored visually with a 4X microscope objective until a fine point was observed. The other end of the fiber entered the fluorometer sample compartment through a curtain of blackout material (Thorlabs) and was attached to the SMA connector. With this instrumentation, the fiber acted as light guide for both excitation and emission light.

A shear apparatus was constructed from a glass pipette (2 ml volume, inner diameter 4 mm) attached to a side hole that was drilled into a small (30 ml) plastic container. The fiberoptic tip was guided into the pipette through a second hole on the opposite side to the pipette. The tip was placed at 20 mm distance from the end of the pipette in order to stay in a region of undisturbed flow. The fiber was then supported outside of the container to prevent lateral movement, and to center the tip with respect to the pipette. Silicone seals prevented leaking of the fluid. A sketch of the shear apparatus can be found in Figure 1. The other end of the pipette was connected to a computer-controlled syringe pump to deliver defined flow rates and flow profiles.

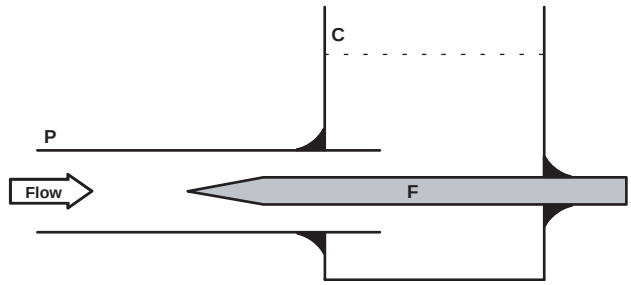

Fig. 1. Sketch of the fiberoptic shear apparatus. The optical fiber F with an etched tip was placed in the center of a glass pipette P. A small plastic container C served as fluid repository and also held the pipette and the fiber in position. The tip was inserted 20 mm upstream of the pipette end to keep it in an undisturbed flow region. Flow was applied to the far end of the pipette by means of a syringe pump.

2.2. Fluid Preparations

Three molecular rotors were examined: 9-(2,2-dicyanovinyl)-julolidine (DCVJ) and 9-(2-carboxy-2-cyanovinyl)-julolidine (CCVJ) purchased from Helix Research, Springfield, OR; and CCVJ-triethyleneglycol ester (CCVJ-TEG) synthesized by our group.[17] Figure 2 shows the chemical structures of the compounds. The difference is the presence of a functional group (COOH in the case of CCVJ and triethyleneglycol in the case of CCVJ-TEG) that defines solvent interaction, primarily water-solubility.[17] Viscous fluids were prepared from mixtures of methanol, ethylene glycol and glycerol (Sigma, St. Louis, MO). Each of the mixtures was stained with one fluorescent molecular rotor at a concentration of 10 μM. Additional fluids were prepared with fluorescein at the same concentration. Fluorescein is not a molecular rotor and therefore serves as control.

Each of the fluids was filled into a 30 ml syringe that was placed on the syringe pump. The pipette was carefully

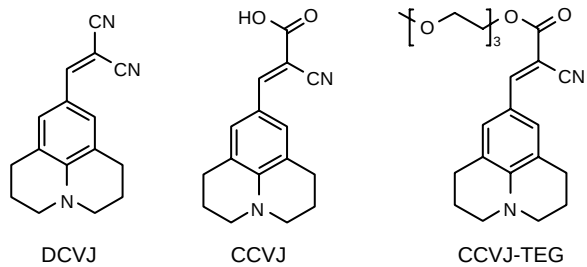

Fig. 2. Chemical structures of the three rotors examined.

filled to avoid air bubbles. Flow profiles were generated under computer control as follows: After obtaining the intensity baseline at no flow for 1 minute, flow was turned on for 30 seconds and paused for 1 minute, then turned on at the next higher level and so on, until a sequence of 0 ml/min, 0.05 ml/min, 0.1 ml/min, 0.25 ml/min, 0.5 ml/min, 0.75 ml/min, 1 ml/min, 2.5 ml/min, 5 ml/min, 7.5 ml/min, and 10 ml/min was completed, covering a flow range over a factor of 200. In the case of water, flow rates of 0.05 ml/min and 0.1 ml/min were omitted. Differences were computed from the average intensities over the 30 seconds of flow minus the average baseline intensity.

2.3. Statistical Analysis

Each experiment was performed in triplicate with the exception of the matrix experiments (intensity increase as a function of shear rate and viscosity), where experiments were repeated four times. Error bars show mean value ± SD. In the stirrer experiments, the t-test was used to determine if averaged intensity during the stirring period was statistically different from averaged intensity before stirring. Flow-dependent intensity increase was computed by averaging emission intensity during the flow period and subtracting averaged intensity of the no-flow period before and after flow application. The resulting data (intensity increase ΔI over flow rate) were analyzed using the one-sample t-test to test whether ΔI was significantly different from zero for a specific flow rate. One-way ANOVA was performed on the complete data set. A post-test for linear trend was performed to determine the significance of the overall increasing trend, while Bonferroni's multiple comparison test provided information on the difference of neighboring ΔI. Statistical analysis was performed using Graphpad Prism version 4.00 (Graphpad Inc., San Diego). Significance was assumed at $p < 0.05$.

3. RESULTS

3.1. Basic Behavior of Molecular Rotors in Sheared Fluids

Molecular rotors featuring a functional group, CCVJ and CCVJ-TEG, showed a marked increase in emission intensity when the fluids were sheared. Figure 3 allows the comparison of the emission spectra of CCVJ in a cuvette without fluid motion and when stirred. A 20% increase in peak emission intensity was observed. A similar, but lower (7%), increase was observed with CCVJ-TEG. In three independent experiments for each dye, this increase was statistically significant ($p < 0.05$). Neither fluorescein nor DCVJ exhibited any increase in emission intensity (Fig. 4) under the same conditions.

In the fiberoptic-based flow apparatus, a similar intensity increase was observed. Emission spectra of 10 μM CCVJ in ethylene glycol in the presence and absence of flow can be seen in Figure 5. Peak intensity increased by about 10% under the application of 1 ml/min flow, which corresponds to a fluid velocity of 2.7 mm/s in the center of the tube. This increased emission intensity was not observed in three control fluids, (1) ethylene glycol without any fluorescent dye, (2) ethylene glycol with 10 μM fluorescein, which is not a molecular rotor, and (3) ethylene glycol with 10 μM DCVJ, a hydrophobic molecular rotor without hydrophilic functional groups.

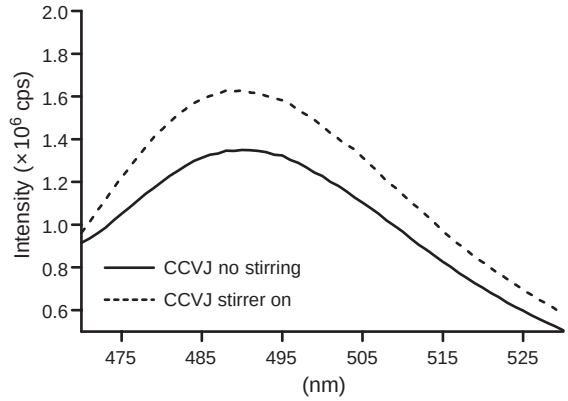

Fig. 3. Emission spectra of 10 μM CCVJ in ethylene glycol, taken in a fluorometer cuvette with and without stirring.

Intensity increase was higher with higher flow rates in a dose-response fashion. Figure 6 shows a representative time-course of emission intensity in response to flow. It can be seen that a statistically significant increase over the no-flow intensity level is achieved at flow rates as low as 0.25 ml/min. For flow rates of 0.05 ml/min and 0.1 ml/min, ΔI was not significantly different from zero. An overall linear trend of ΔI was observed with increasing flow rates ($p < 0.0001$). ΔI at flow rates of 5 ml/min, 7.5 ml/min, and 10 ml/min were not statistically different

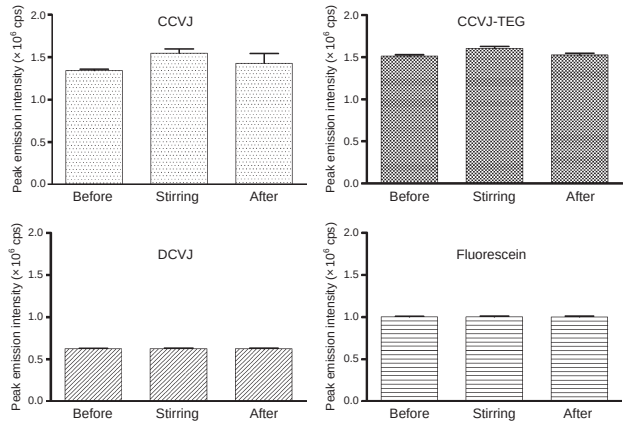

Fig. 4. 10 μM CCVJ in ethylene glycol in a fluorometer cuvette before the stirrer was activated, during, and after stirring. Slow stirring increases both CCVJ and CCVJ-TEG intensity significantly (t-test, $p < 0.05$) over unstirred control. Two control dyes, DCVJ and fluorescein do not show this increase (t-test, n.s.).

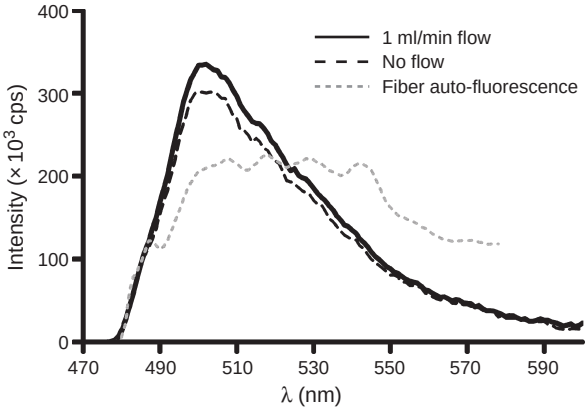

Fig. 5. Background-corrected fluorescence emission spectrum of 10 μM CCVJ in ethylene glycol without flow and at 1 ml/min flow. Spectroscopy indicates that emission intensity increases with flow. No spectral shifts were observed. The background signal (fiber immersed in ethylene glycol without dye) that was subtracted from the dye spectra is shown as grey dotted line.

from each other. Figure 7 shows a timecourse experiment with DCVJ in ethylene glycol. No increase in emission intensity was observed. The water-soluble dyes CCVJ and CCVJ-TEG were also tested in water. While CCVJ-TEG failed to exhibit an intensity increase under shear in water, the effect could clearly be observed with CCVJ (Fig. 8). Consistent with the lower viscosity of water relative to ethylene glycol, the intensity increase was markedly lower. No measurable intensity increase was observed with flow rates of 0.1 ml/min and below. At flow rates of 0.5 ml/min and above, ΔI was significantly different from zero. In addition, a significant linear trend of ΔI over flow was observed ($p < 0.0001$).

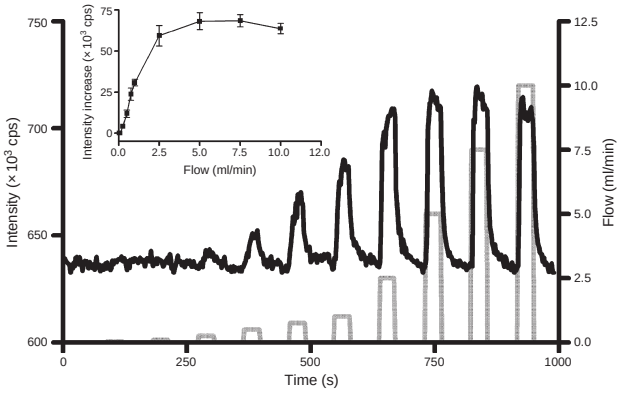

Fig. 6. Representative timecourse experiment where emission intensity of 10 μM CCVJ in ethylene glycol was monitored at fixed excitation and emission wavelengths. Flow was increased over a wide range (factor of 200). Inset shows the averaged intensity over baseline during periods of flow as a function of the applied flow rate. Application of flow leads to an increased emission intensity in a dose-response fashion, but no significant increase was seen below 0.05 and 0.1 ml/min, and an apparent saturation effect (no further increase of intensity) becomes visible above 5 ml/min. The apparent (and nonsignificant) decrease of intensity at 10 ml/min may be attributed to unstable flow conditions.

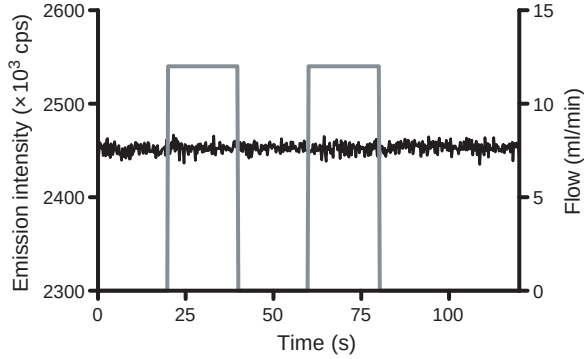

Fig. 7. Timecourse experiment using 10 μM DCVJ in ethylene glycol. As opposed to both CCVJ and CCVJ-TEG, no changes in intensity were observed, in spite of relatively high flow rates.

3.2. Differentiation Between Shear Rate and Shear Stress

In order to differentiate between shear rate and shear stress effects, timecourse experiments were repeated with the same flow profile, but with fluids of different viscosity. It can be seen in Figure 9 that intensity increases occur with both increased flow and increased viscosity. This effect was observed with both CCVJ and CCVJ-TEG. In both cases, the response (differential intensity increase) was higher at low flow rates and low viscosities.

3.3. Possible Applications as Flow and Shear Sensors

Flow velocity in a cylindrical tube exhibits a parabolic profile $v(r)$ following Eq. 1,

$$v(r) = V_{\max} \cdot \left(1 - \frac{r^2}{R^2}\right) \qquad (1)$$

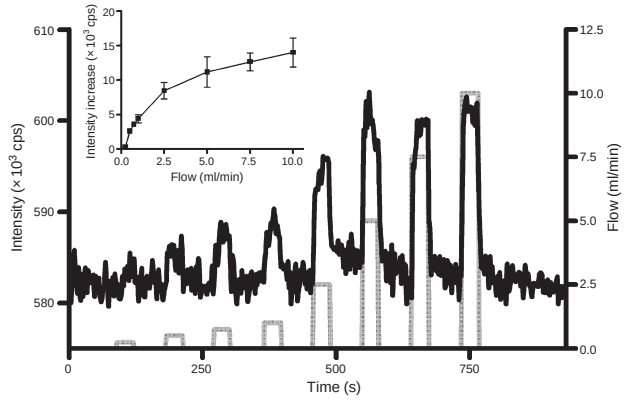

Fig. 8. Representative timecourse experiment where emission intensity of 10 μM CCVJ in water was monitored at fixed excitation and emission wavelengths. Flow was increased from 0.25 ml/min to 10 ml/min. Inset shows the averaged intensity during periods of flow as a function of the applied flow rate. Similar to the experiment in ethylene glycol (Fig. 6), application of flow lead to an increased emission intensity in a dose-response fashion. Higher flow rates than 5 ml/min did not lead to significantly higher emission intensities.

RESEARCH ARTICLE

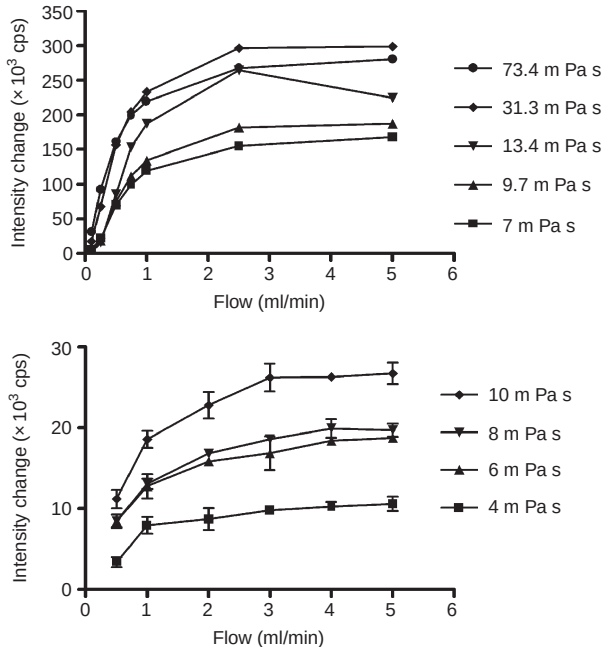

Fig. 9. Matrix experiment where intensity increase was observed at different flow rates in fluids of different viscosities (mixtures of ethylene glycol and glycerol). Shown are the dyes CCVJ (left) in a single experiment and CCVJ-TEG (right) as means and SD of four experiments. Intensity increase can be seen with both flow and viscosity, indicating that the effect is based on shear stress rather than shear rate.

where V_{max} is the flow velocity in the center of the tube, and R is the tube radius.[18] By changing the position of the fiber tip relative to the wall, the tip was exposed to different flow velocities. As the tip was placed closer to the wall, a less pronounced intensity increase was observed (Fig. 10). As can be seen in Figure 10, the intensity increase follows closely the expected parabolic profile with a maximum in the tube center and a minimum close to the tube wall ($R^2 = 0.98$). Deviation of the data values from the model were not significant (runs test, $p = 0.84$), indicating that the parabolic model is applicable to describe the data.

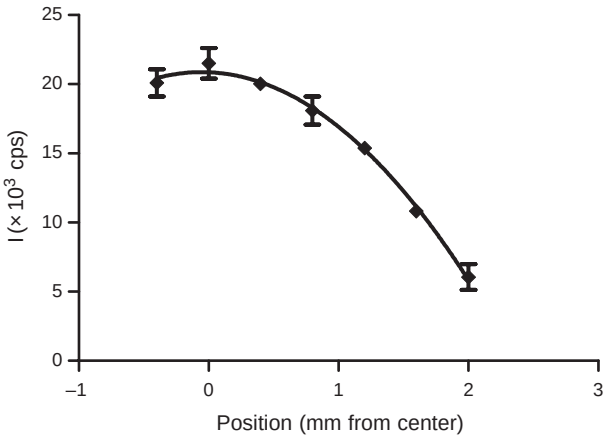

Fig. 10. Intensity increase caused by constant flow but with varying radial position of the fiber tip in a cylindrical tube. Shown is means ± SD of three experiments. Maximum intensity increase was seen in the tube center, with a marked reduction towards the tube wall. A parabolic profile, following the flow velocity equation in a cylinder (Eq. 1), shows an excellent fit into the data.

4. DISCUSSION

In this study, we have demonstrated a new effect related to molecular rotors—an increase in emission intensity related to shear stress that the solvent experienced. Fluids with specific molecular rotors dissolved in them showed increased fluorescence emission if exposed to fluid flow. Prerequisite for this effect was the presence of a hydrophilic functional group, which is the case for CCVJ and CCVJ-TEG. Intensity increases were not seen in fluids without any fluorescent dye, in fluids with a fluorescent dye that is not a molecular rotor (fluorescein) and in fluids that contain a molecular rotor (DCVJ) that lacks functional groups. These observations point at a crucial role of the functional group. Since the observed effects may potentially be attributed to photobleaching, we measured photobleaching under no-flow conditions and did not find any measurable fluorescence decrease over a 10-minute period in either the cuvette or fiber experiment. This is to be expected, because excitation light intensity is relatively low in the fluorometer experiments. We therefore conclude that photobleaching does not play a role in these experiments.

Figure 5 allows the comparison of emission spectra with and without flow. The increased emission can clearly be seen, but there was no spectral shift, indicating that the polarity of the environment does not change. It can also be seen that the magnitude of the change is relatively small. This may be attributed to fiber autofluorescence: The fiber itself contributes to the fluorescence by emitting green light when acting as a guide for blue excitation light. This side effect was observed in several different fibers and was related to the cladding. The intrinsic emission of the fiber is stronger than the dye fluorescence, reducing the measurable relative intensity change. We expect an improvement by modifications of the shear apparatus, but primarily by using suitable fibers custom-designed for minimum fluorescence in the green range. With the present apparatus, however, significant intensity increase was seen at flow rates as low as 0.25 ml/min, which corresponds to a fluid velocity of 0.6 mm/s in the center of the tube. This indicates that molecular rotors acting as shear sensors have very high sensitivity.

This high sensitivity may also be the primary cause of the exponential decay of intensity after cessation of flow. By adding elastic tubing to the experimental apparatus, the decay constants became longer due to tubing elasticity (data not shown). Pinching of the elastic tubing with a finger causes a measurable spike in fluorescence intensity.

Unfortunately, no flow apparatus exists to our knowledge that allows measurement of such low flow rates, therefore it was not possible to directly relate flow at the fiber tip to fluorescence intensity.

On the other hand, differential intensity increase (intensity increase per unit increase of flow) was reduced at high flow rates (Fig. 6). This effect may be interpreted either as saturation or as the intrinsic response of the dye molecules. If those molecules exposed to the highest shear stress reach a quantum yield of unity, further increase of emission intensity is not possible, leading to a saturation effect. Since the exact sensing mechanism is as yet unknown, it is also conceivable that the natural response of the dye may best be modeled by an exponential relation (Eq. 2),

$$\Delta I = \Delta I_{\max} \cdot \left(1 - \exp\left(-\frac{v}{v_c}\right)\right) \quad (2)$$

where the measurable intensity increase ΔI depends on the maximum intensity increase $\Delta I_{\max}$, a constant characteristic flow velocity v_c, and the fluid velocity v. At very high flow rates, the flow apparatus itself may pose limitations. Undisturbed flow in the tube should be in the laminar range with Reynolds numbers in the order of 50 and below in all experiments. However, the introduction of the tip may cause disturbed flow at high flow rates, particularly, if the tip is not perfectly smooth. The increased noise that was observed in the intensity values at high flow rates may be attributed to this effect.

In experiments involving both changes in shear rate and viscosity (Fig. 9), we found that the observed intensity increase depends on both. Shear rate is the velocity gradient in the fluid. Since shear stress τ is the product of viscosity η and shear rate γ, we conclude that shear stress, rather than shear rate, is the determinant of the intensity increase. The simple model (Eq. 3)

$$\Delta I \propto \tau = \eta \cdot \gamma \quad (3)$$

does not account for saturation effects at high shear stress values. Values for τ and ΔI correlate only at $R^2 = 0.68$. Omitting the data values at 5 ml/min and 73 m Pa s increased this correlation to $R^2 = 0.84$. A purely empirical curve fit into the present data yields Eq. 4,

$$\Delta I = \Delta I_{\max} \cdot \left(1 - \exp\left(-\frac{\eta}{\eta_c}\right)\right) \cdot \left(1 - \exp\left(-\frac{v}{v_c}\right)\right) \quad (4)$$

where the intensity increase follows both fluid velocity v (with a characteristic constant velocity v_c) and viscosity (with a constant characteristic viscosity η_c) in an exponential relaxation fashion with $R^2 = 0.97$. However, there is no physical rationale at this time to prefer one over the other model. Either model, however, is markedly different from the relationship of intensity with viscosity in unsheared fluids, known as the Förster-Hoffmann-equation (Eq. 5),

$$I \propto C \cdot \eta^x \quad (5)$$

where I is the measured emission intensity, C is a temperature-dependent constant, and x is a dye-dependent constant, which is usually in the range of 0.6.[3, 11]

In Figure 10, the primary determinant of intensity increase is fluid velocity. This is not a contradiction with the notion that the intensity increase is determined by shear stress, because the volume in which fluorescence emission is acquired is very small. The intensity of an evanescent wave at the surface of a fiberoptic tip decays very rapidly with the distance of the tip.[19, 20] The 1/e distance of the evanescent wave was less than 200 μm in our experimental setup. Consequently, emission intensity is acquired only inside a very thin layer at the tip surface. Shear stress is therefore dominated by fluid friction at the tip surface rather than the parabolic flow gradient of the tube. This fluid friction, in turn, is determined by the local flow velocity close to the tip, rather than the global shear stress in the tube. A larger excitation volume may be created by using external laser beams rather than using the optical fiber as a conduit for excitation light. Including a larger measurement volume would reduce the effects of flow profile distortion at the fiber tip. A more effective means of differentiating between flow and shear stress would be the inclusion of a viscosity-sensitive probe that does not exhibit shear sensitivity, such as DCVJ. By obtaining local viscosity and local shear stress, local shear rate could be determined.

Based on the data presented, we speculate that the underlying mechanism is based on polar solvent-dye interaction, primarily mediated by the functional groups. The interaction of fluorescent dyes with polar solvents has been intensively studied. Generally, polar interaction causes molecular reorientation in the excited state of the fluorophore. This interaction can be observed through a spectral red-shift and reduced emission intensity. The underlying dynamic processes are very complex and not yet fully explored.[21] In molecular rotors, an additional effect takes place: They return to the ground state from the excited state either through fluorescence emission or through intramolecular rotation without fluorescence emission. This behavior has been studied in relation to the viscosity of the solvent.[3–5] The relationship between intensity and viscosity has been explained by the deexcitation rates. In the case of DCVJ, the radiative decay rate is 2.78×10^8 sec^{-1}, while the nonradiative (rotational) decay rate is about three orders of magnitude higher ($\approx 10^{11}$ sec^{-1}) and strongly viscosity-dependent.[22] Since the fluorescent quantum yield is defined as the ratio of fluorescent deexcitation events to total deexcitation events, the quantum yield of molecular rotors becomes viscosity-dependent. A power-law relationship between viscosity and quantum yield has been found.[3, 6] Under steady-state conditions, this behavior relates to increased emission intensity with increased solvent viscosity. Although the molecular rotors used in this study are known to exhibit some emission shift with

RESEARCH ARTICLE

changes in the polarity of the environment, the effects have been separated: Viscosity influences quantum yield, while polarity induces a minor spectral shift.[7] The additional effect of fluid shear stress on this complex interaction is widely unknown, but it is conceivable that fluid flow alters the reorientation due to the much higher internal friction forces of the fluid. Additional studies involving different functional groups as well as different polarity-sensitive probes are required to fully elucidate the underlying mechanism, particularly how fluid shear stress influences the molecular rotor's internal reorientation rate.

In conclusion, we present a novel behavior of molecular rotors that may enable them to be used as sensitive sensors for flow and shear stress in aqueous and other polar media. Due to the small size it is conceivable that molecular rotors may be developed into nanoscale sensors for flow profiles in microfluidics or the microvasculature. In addition, the high sensitivity of the sensor extends the capabilities of flow sensors into the low-flow range. A fiberoptic-based sensor may be used *in-vivo*, where not only its sensitivity is an advantage, but also the low cost of the instrumentation when compared to other *in-vivo* modalities, such as Doppler ultrasound or magnetic resonance imaging. On the other hand, the use of a fiberoptic probe must be considered an invasive technique, and a considerable development effort may be required to obtain the fluorescence signals through blood vessel walls. When used to determine shear stress, the use of fluorescent measurements poses great advantages over the purely mechanical determination of shear stress which involves introducing small bodies into the flow and measuring the drag.

Acknowledgments: This study was in part funded by the National Institutes of Health, grant 1R21-RR018399.

References and Notes

1. Z. R. Grabowski, K. Rotkiewicz, and W. Rettig, *Chem. Rev.* 103, 3899 **(2003)**.
2. K. Rotkiewicz, K. H. Grellmann, and Z. R. Grabowski, *Chem. Phys. Lett.* 19, 315 **(1973)**.
3. Th. Förster and G. Hoffmann, *Z. Phys. Chem.* 75, 63 **(1971)**.
4. R. O. Loutfy and B. A. Arnold, *J. Phys. Chem.* 86, 4205 **(1982)**.
5. K. Y. Law, *Chem. Phys. Lett.* 75, 545 **(1980)**.
6. C. E. Kung and J. K. Reed, *Biochemistry* 25, 6114 **(1986)**.
7. M. L. Viriot, M. C. Carré, C. Geoffroy-Chapotot, A. Brembilla, S. Muller, and J.-F. Stoltz, *Clin. Hemorheol. Microcirc.* 19, 151 **(1998)**.
8. T. Furuno, R. Isoda, K. Inagaki, T. Iwaki, M. Noji, and M. Nakanishi, *Immunol. Lett.* 33, 285 **(1992)**.
9. C. E. Kung and J. K. Reed, *Biochemistry* 28, 6678 **(1989)**.
10. T. Iio, S. Takahashi, and S. Sawada, *J. Biochem.* 113, 196 **(1993)**.
11. M. A. Haidekker, A. G. Tsai, T. Brady, H. Y. Stevens, J. A. Frangos, E. Theodorakis, and M. Intaglietta, *Am. J. Physiol. Heart Circ. Physiol.* 282, H1609 **(2002)**.
12. D. Liepsch, *J. Biomech.* 35, 415 **(2002)**.
13. Y. Sugii, S. Nishio, and K. Okamoto, *Ann. N. Y. Acad. Sci.* 972, 331 **(2002)**.
14. N. Resnick, H. Yahav, A. Shay-Salit, M. Shushy, S. Schubert, L. C. Zilberman, and E. Wofovitz, *Prog. Biophys. Mol. Biol.* 81, 177 **(2003)**.
15. D. P. Giddens, C. K. Zarins, and S. Glagov, *J. Biomech. Eng.* 115, 588 **(1993)**.
16. C. H. Turner and F. M. Pavalko, *J. Orthop. Sci.* 3, 346 **(1998)**.
17. M. A. Haidekker, T. P. Brady, S. H. Chalian, W. Akers, D. Lichlyter, and E. A. Theodorakis, *Bioorganic Chemistry* 32, 274 **(2004)**.
18. C. J. Geankoplis, in *Transport Processes and Separation Process Principles*, edited by Prentice-Hall, Upper Saddle River **(2003)**, p. 34.
19. J. J. Janata, in *Principles of Chemical Sensors*, Plenum Press, New York **(1989)**, p. 251.
20. J. P. Golden, G. P. Anderson, S. Y. Rabbany, and F. S. Ligler, *Trans. Biomed. Eng.* 41, 585 **(1994)**.
21. J. R. Lakowicz, in *Principles of Fluorescence Spectroscopy*, edited by Kluwer Academic/Plenum Publishers, New York **(1999)**, p. 211.
22. R. O. Loutfy and K. Y. Law, *J. Phys. Chem.* 84, 2803 **(1980)**.